ρ-ω Interference and the ω-ϕ Mixing Angle*

RONALD G. PARSONS
Center for Particle Theory, Department of Physics, The University of Texas, Austin, Texas 78712
(Received 11 August 1969)

The ω-ϕ mixing angle of $SU(3)$ is usually assumed to be positive, but only its magnitude is actually determined by various models of $SU(3)$ breaking. The effect of this ambiguity of the relative sign of the $SU(3)$ prediction of the γ-ρ and γ-ω coupling constants on ρ-ω interference is investigated. The interference can be "constructive" or "destructive." In photoproduction of lepton pairs, destructive interference causes the effect of ρ-ω interference to be smaller than that of previous calculations. Two new models of ρ-ω interference in the colliding-beam reaction $e^+ + e^- \to \pi^+ + \pi^-$ are discussed. A measurement of the cross section for the latter reaction would make possible a determination of the sign of the ω-ϕ mixing angle.

I. INTRODUCTION

THE eightfold way,[1] vector-meson dominance[2] (VMD), and various models of $SU(3)$ breaking[3] give predictions for the relative coupling strengths of the photon to the ρ, ω, and ϕ mesons. The theories, unfortunately, do not predict the relative *sign* of the γ-ρ and γ-ω coupling constants. For example, the Gell-Mann–Okubo mass formula,[4] when applied to the squares of the ρ, ω, and ϕ masses, predicts an ω-ϕ mixing angle of $\sin\theta \approx \pm 1/\sqrt{3}$. This gives us the famous 9:1:2 ratios for the squares of the coupling constants of the photon to the ρ, ω, and ϕ mesons, but makes no definite prediction for the signs of the coupling constants themselves. The VMD theory of LKZ[2] contains two mixing angles, θ_Y and θ_N. Various models of $SU(3)$ breaking have been postulated to give predictions for these angles but they do not predict the *sign* of θ_Y. It is usually *assumed* to be positive.

In this paper, we investigate the consequences of this sign ambiguity on ρ-ω interference in the photoproduction of lepton pairs and in e^+e^- colliding-beam experiments. The relative sign of the γ-ρ and γ-ω coupling constants enters directly in the amplitudes for $e^+e^- \to \rho \to \pi^+\pi^-$ and $e^+e^- \to \omega \to \pi^+\pi^-$. The interference between the ρ and ω depends strongly on this sign. In the photoproduction of lepton pairs, the process can proceed through the "Compton graphs," i.e., first a vector meson is photoproduced and subsequently decays into a lepton pair. At symmetry in the lepton angles and energies, the "Compton graphs" do not interfere with the pure quantum-electrodynamic Bethe-Heitler process in lowest order. The relative phase of the $\gamma + A \to \rho + A$ and $\gamma + A \to \omega + A$ amplitudes, where A is the nuclear target, can also depend on the relative sign of the γ-ρ and γ-ω coupling constants. Previous calculations[5] of ρ-ω interference in this process have assumed that the relative phase was near zero.

In Sec. II, the effect of the interference of the $\rho \to 2\pi$ channel with the $\omega \to 2\pi$ channel in an e^+e^- colliding-beam experiment is considered and, in Sec. III, ρ-ω interference in photoproduction of lepton pairs is discussed.

II. COLLIDING-BEAM EXPERIMENTS

Colliding-beam experiments where the reaction $e^+e^- \to \pi^+ + \pi^-$ is measured can be affected by ρ-ω interference. The interference in this case is due to the small, but nonzero, amplitude for the ω meson to decay into two pions. There are several models one can use to calculate this effect. Fortunately the predictions of the different models are quite different and, if data were taken with total center-of-mass energy near $m_\omega c^2$, it would be easy to distinguish which model was more nearly correct. The photon (γ)–vector-meson (V) coupling constant will be taken as

$$g_{V\gamma} = -e m_V^2 / 2\gamma_V . \tag{1}$$

The magnitude of the coupling constant γ_V in Eq. (1) can be determined from the leptonic decay widths for the vector mesons. Neglecting terms of the order of $(m_l/m_V)^4$, these are given by[2]

$$\Gamma(\rho \to l^+l^-) = \tfrac{1}{12}\alpha^2 (\gamma_\rho^2/4\pi)^{-1} m_\rho , \tag{2a}$$

$$\Gamma(\omega \to l^+l^-) = \tfrac{1}{12}\alpha^2 (\gamma_Y^2/4\pi)^{-1} \sin^2\theta_Y \, m_\omega = \tfrac{1}{12}\alpha^2 (\gamma_\omega^2/4\pi)^{-1} m_\omega , \tag{2b}$$

$$\Gamma(\phi \to l^+l^-) = \tfrac{1}{12}\alpha^2 (\gamma_Y^2/4\pi)^{-1} \cos^2\theta_Y \, m_\phi = \tfrac{1}{12}\alpha^2 (\gamma_\phi^2/4\pi)^{-1} m_\phi . \tag{2c}$$

The coupling constant of the octet central member ϕ_8 to the hypercharge current is γ_Y, the ω-ϕ mixing angle is θ_Y, and α is the fine structure constant.

The recent Orsay results[3] for the partial widths of the vector mesons are

$$\Gamma(\rho \to e^+e^-) = 7.36 \pm 0.70 \text{ keV} ,$$
$$\Gamma(\omega \to e^+e^-) = 0.94 \pm 0.18 \text{ keV} ,$$
$$\Gamma(\phi \to e^+e^-) = 1.64 \pm 0.24 \text{ keV} .$$

* Supported in part by the National Science Foundation.

[1] See M. Gell-Mann and Y. Ne'eman, *The Eightfold Way* (W. A. Benjamin, Inc., New York, 1964).

[2] J. J. Sakurai, Ann. Phys. (N. Y.) **11**, 1 (1960); N. Kroll, T. D. Lee, and B. Zumino, Phys. Rev. **157**, 1376 (1967). The latter paper is hereafter referred to as KLZ.

[3] A recent tabulation of theoretical and experimental results and references is given by J. E. Augustin *et al.*, Phys. Letters **28B**, 503 (1969).

[4] M. Gell-Mann, Phys. Rev. **125**, 1067 (1962); S. Okubo, Progr. Theoret. Phys. (Kyoto) **27**, 949 (1962).

[5] R. G. Parsons and R. Weinstein, Phys. Rev. Letters **20**, 1314 (1968); M. Davier, Phys. Letters **27B**, 27 (1968).

From these data, one finds

$$\gamma_\rho^{-2}:\gamma_\omega^{-2}:\gamma_\phi^{-2}=9:(1.28\pm0.25):(1.72\pm0.27). \quad (3)$$

The unbroken $SU(3)$ predictions using $\sin^2\theta=\frac{1}{3}$ are

$$\gamma_\rho^{-2}:\gamma_\omega^{-2}:\gamma_\phi^{-2}=9:1:2.$$

Thus the values in Eq. (3) are not in disagreement with unbroken $SU(3)$. The predictions of other theories may be found in Ref. 3.

In the discussion below, we use the following values for the photon–vector-meson coupling constants obtained from the Orsay experiments:

$$\gamma_\rho^{-1}:\gamma_\omega^{-1}:\gamma_\phi^{-1}=3:\pm1.13:1.31. \quad (4)$$

The relative sign of γ_ω^{-1} in Eq. (4) is to be determined by experiment. Two models for the reaction $e^++e^-\rightarrow\pi^++\pi^-$ will be discussed below.

The first model is similar to one propsoed by Greenberg.[6] In this model, it is assumed that the $\omega\rightarrow2\pi$ decay may be represented by the diagram in Fig. 1(a). In other words, there is some coupling,[7] perhaps electromagnetic, between the ω and ρ that allows an isospin (G-parity) change. Phenomenologically, the coupling constant $m_{\omega\rho}^2$ can be adjusted to fit the observed partial width $\Gamma(\omega\rightarrow2\pi)$. The presence of the ρ propagator acts as a ρ-dominance form factor for the $\omega\pi\pi$ vertex. When the amplitudes corresponding to Figs. 1(a) and (1c) are added and then squared, the differential cross section is given by

$$\frac{d\sigma}{d\Omega}=\frac{\alpha^2\beta_\pi^3(1-\cos^2\theta)}{32E^2}|F(E)|^2,$$

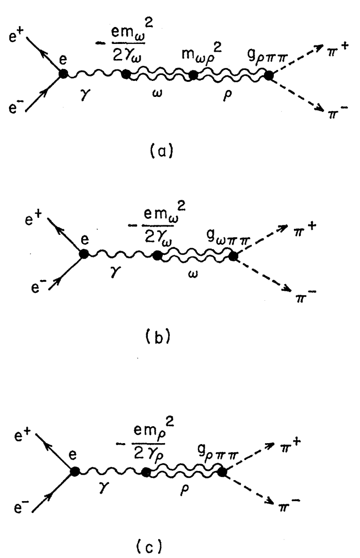

FIG. 1. Feynman diagrams: (a) for $e^++e^-\rightarrow\pi^++\pi^-$ via the $\omega\rightarrow2\pi$ channel; (b) for $e^++e^-\rightarrow\pi^+\pi^-$ via the $\omega\rightarrow2\pi$ channel; (c) for $e^++e^-\rightarrow\pi^++\pi^-$ via the $\rho\rightarrow2\pi$ channel.

[6] D. F. Greenberg, Nuovo Cimento 38, 1908 (1965).
[7] L. E. Picasso *et al.*, Nuovo Cimento 37, 187 (1965).

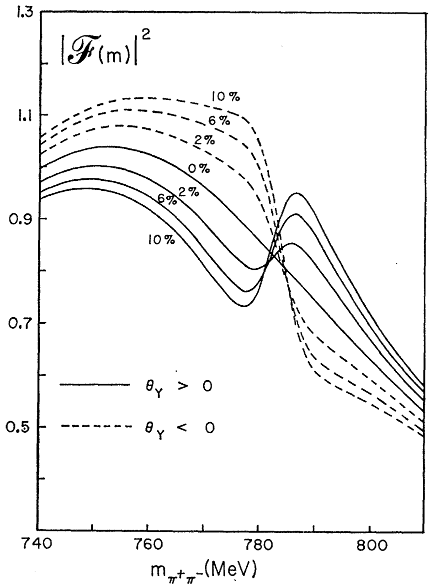

FIG. 2. Graph of the function $|\mathfrak{F}(m)|^2$ [see Eq. (5)]. The mode used is that of Figs. 1(a) and 1(c). The masses and widths are $m_\rho=765$ MeV, $m_\omega=783.4$ MeV, $\Gamma_{\rho\pi\pi}=125$ MeV, and $\Gamma_\omega=12.6$ MeV. The percentages given correspond to $\Gamma_{\omega\pi\pi}/\Gamma_{\omega3\pi}$.

where β_π is the velocity of the pions and E is the initial electron energy. The pion-electromagnetic form factor $F(E)$ will be dominated by the ρ resonance for $E\approx\frac{1}{2}m_\rho$. The magnitude of $|F(E)|^2$ at $E=\frac{1}{2}m_\rho$ depends on the model one uses to calculate $F(E)$, e.g., how one includes the correct analytic behavior of the form factor. Since our main interest in this paper is in deviations from the pure ρ-dominance model [see Fig. 1(c)] near the ρ mass, we arbitrarily normalize $|F(E)|^2$ to unity at $E=\frac{1}{2}m_\rho$ in the absence of any contribution of the ω meson. We denote this "normalized" form factor by $\mathfrak{F}(m)$ where $m=2E$.

The form factor squared $|\mathfrak{F}(m)|^2$ resulting from adding the amplitudes corresponding to Figs. 1(a) and 1(c) is given by

$$|\mathfrak{F}(m)|^2=\left|\frac{m_\rho\Gamma_\rho(m_\rho)}{m^2-m_\rho^2+im_\rho\Gamma_\rho(m)}\right|^2$$

$$\times\left|1+\frac{m_\omega^2}{m_\rho^2}\frac{\gamma_\omega^{-1}}{\gamma_\rho^{-1}}\frac{m_{\omega\rho}^2}{m^2-m_\omega^2+im_\omega\Gamma_\omega}\right|^2, \quad (5)$$

where

$$\Gamma_\rho(m)=\frac{m_\rho}{m}\left(\frac{m^2-4m_\pi^2}{m_\rho^2-4m_\pi^2}\right)^{3/2}\Gamma_{\rho\pi\pi}. \quad (6)$$

A plot of $|\mathfrak{F}(m)|^2$ for various values of $\Gamma_{\omega\pi\pi}/\Gamma_{\omega3\pi}$, i.e., for various values of $m_{\omega\rho}^2$, is shown in Fig. 2. Curves for both positive and negative ratios of $\gamma_\omega^{-1}/\gamma_\rho^{-1}$ are shown. In Ref. 6 a positive ratio was assumed. The results for the different relative signs of the photon–vector-meson coupling constants are significantly different.

The second model consists of adding the amplitudes corresponding to Figs. 1(b) and 1(c). This corresponds to a constant $\omega\pi\pi$ form factor. The form factor squared $|\mathfrak{F}(m)|^2$ resulting from this model is given by

$$|\mathfrak{F}(m)|^2 = m_\rho^2\Gamma_\rho(m_\rho)^2 \left| \frac{1}{m^2-m_\rho^2+im_\rho\Gamma_\rho(m)} + \frac{m_\omega^2}{m_\rho^2}\frac{\gamma_\omega^{-1}}{\gamma_\rho^{-1}}\frac{g_{\omega\pi\pi}}{g_{\rho\pi\pi}}\frac{1}{m^2-m_\omega^2+im_\omega\Gamma_\omega}\right|^2, \quad (7)$$

where $g_{\omega\pi\pi}$ is adjusted to fit the observed partial width $\Gamma_{\omega\pi\pi}$. A plot of $|\mathfrak{F}(m)|^2$ calculated using this model for various values of $\Gamma_{\omega\pi\pi}/\Gamma_{\omega3\pi}$ is shown in Fig. 3. Curves for both positive and negative ratios of $\gamma_\omega^{-1}/\gamma_\rho^{-1}$ are shown. This model appears similar to that of Donnachie[8] and gives similar results for $\gamma_\omega^{-1}/\gamma_\rho^{-1}$ positive.

The results of the two models discussed above for $\gamma_\omega^{-1}/\gamma_\rho^{-1}$ negative and the models of Greenberg[6] and Donnachie[8] are all quite different. Each model has a unique signature. The model of Greenberg predicts a decrease in the cross section due to ρ-ω interference for m just below m_ω and an increase just above m_ω. The model of Donnachie predicts an increase on both sides of m_ω. For $\gamma_\omega^{-1}/\gamma_\rho^{-1}<0$, the results of Eq. (5) show an increase below and a decrease above m_ω, while the results of Eq. (7) show a decrease on both sides of m_ω. Thus an accurate experiment would enable one to determine the sign of θ_Y and, thus, the sign of $\gamma_\omega^{-1}/\gamma_\rho^{-1}$. In addition, the measurement of the cross section for $e^++e^-\rightarrow\pi^++\pi^-$ near the ω mass enables one to make an accurate measurement of the partial width $\Gamma_{\omega\pi\pi}$.

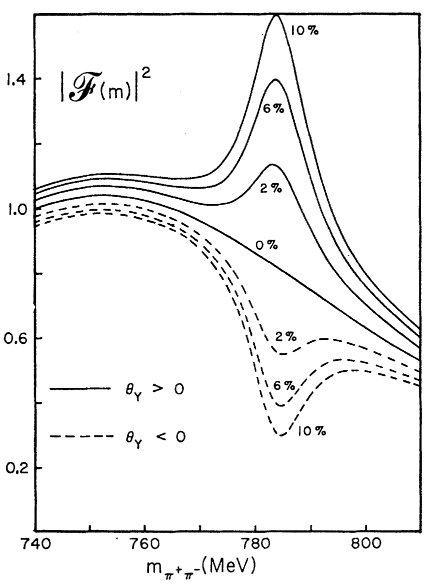

FIG. 3. Graphs of the function $|\mathfrak{F}(m)|^2$ [see Eq. (7)]. The model used is that of Figs. 1(b) and 1(c). The masses and widths are $m_\rho=765$ MeV, $m_\omega=783.4$ MeV, $\Gamma_{\rho\pi\pi}=125$ MeV, and $\Gamma_\omega=12.6$ MeV. The percentages given correspond to $\Gamma_{\omega\pi\pi}/\Gamma_{\omega3\pi}$.

[8] A. Donnachie, Phys. Letters **27B**, 525 (1968).

III. PHOTOPRODUCTION OF LEPTON PAIRS

The highest resolution data to date on leptonic decays of photoproduced vector mesons were obtained by Asbury *et al.*[9] at DESY using a carbon target and a photon energy of ≈ 2.8 GeV. In the rapporteur's summary given by Ting at Vienna in 1968, the following statement was made: "The experiment was done at a low photon energy of 2.7 GeV on a carbon ($T=0$) target, such that the $\omega\rightarrow e^+e^-$ contamination is small. At low energy, the bubble-chamber data show that photoproduction of ω on protons is consistent with OPE. No ω contamination was observed and the measured $\rho\rightarrow e^+e^-$ width is 120 ± 20 MeV/c^2."[10] The experimental mass resolution was ±15 MeV/c^2.

While the hydrogen bubble-chamber data[11] for ω photoproduction are consistent with one-pion exchange (OPE) at low energies, the data are also consistent with a constant total cross section (due to diffraction) of approximately 1.7 μb plus an OPE contribution that varies as $E_\gamma^{-1.6}$. The diffraction and OPE contribution are equal at $E_\gamma\approx4.5$ GeV. Above 2 GeV the hydrogen bubble-chamber data[11] on the ρ photoproduction cross section are fairly constant with energy. This is consistent with pure diffraction production with a total cross section of 16.5 μb. The ratio of the diffraction cross sections is in good agreement with the $SU(3)$ prediction of $\approx 9:1$. Thus, if one eliminates the OPE mechanism for photoproduction by using a $T=0$ target, the amplitude ($A_{\gamma V}$) for diffraction is still nonzero, i.e., $|A_{\gamma\rho}|/|A_{\gamma\omega}| \approx 3/1$. It would, of course, be possible to excite the carbon nucleus to its lowest $T=1$ excited state at 15.1 MeV by OPE. This is an incoherent process and would not interfere with the diffraction production mentioned above.

In the experiment of Ref. 9, the momentum of the photoproduced vector meson was 2.8 GeV/c. The photon energy required to produce this vector meson was therefore slightly in excess of 2.8 GeV. In the following we assume that the ratio of diffraction-photoproduction cross sections for ρ and ω is approximately 9:1 at this photon energy.

In Ref. 5 it was assumed that the relative phase of the amplitude $\gamma\rightarrow\rho\rightarrow e^+e^-$ and $\gamma\rightarrow\omega\rightarrow e^+e^-$ (as measured at the center of each meson resonance) was near zero. In this paper we wish to discuss the effects of this phase difference near 180°, i.e., destructive interference. A possible mechanism for this 180° phase difference is a modification of the vector-dominance model (VDM). One may assume that the interaction takes place as in Fig. 4. This modification of the VDM is made since the present experimental values[10] of $\gamma_\rho^2/4\pi$ appear to depend on whether the process $\gamma\leftrightarrow\rho$ takes place

[9] J. G. Asbury *et al.*, Phys. Rev. Letters **19**, 869 (1967).

[10] S. C. C. Ting, in *Proceedings of the Fourteenth International Conference on High-Energy Physics, Vienna 1968*, edited by J. Prentki and J. Steinberger (CERN, Geneva, 1968), p. 49.

[11] Aachen-Berlin-Bonn-Hamburg-Heidelberg-München Collaboration, Phys. Rev. **175**, 1669 (1968).

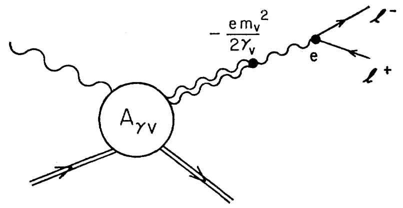

FIG. 4. Revised vector-dominance model for photoproduction of a vector meson and its subsequent decay into a lepton pair.

on the photon mass shell or on the ρ- meson mass shell. By restricting the use of the process $\rho \to \gamma$ to (or near) the ρ-meson mass shell, this uncertainty is eliminated. We calculate the ρ-ω interference by adding two diagrams of this type: one with $V=\rho$, and the other with $V=\omega$. The photon–vector-meson coupling constant appears linearly in the amplitudes. If we assume that the ratio of the vector-meson photoproduction amplitudes for ρ and ω mesons is $A_{\gamma\omega}/A_{\gamma\rho}=+\frac{1}{3}$, and that $\gamma_\omega^{-1}/\gamma_\rho^{-1}$ is negative and given by Eq. (4), we obtain destructive ρ-ω interference. Of course, there are other possible mechanisms for the phase difference. It is possible that $\gamma_\omega^{-1}/\gamma_\rho^{-1}>0$ and $A_{\gamma\omega}/A_{\gamma\rho}=\frac{1}{3}e^{i\theta}$ with θ near 180°. It should be noted that small variations of the phase angle θ of $\approx 30°$ cause small changes in the results below.

Using the model shown in Fig. 4, we find that the excess yield of symmetric lepton-pair events over the pure quantum-electrodynamic prediction is proportional to

$$Y(m)=m_\rho^2\Gamma_\rho(m_\rho)^2\left|\frac{1}{m^2-m_\rho^2+im_\rho\Gamma_\rho(m)} + \frac{A_{\gamma\omega}}{A_{\gamma\rho}}\frac{m_\omega^2}{m_\rho^2}\frac{\gamma_\omega^{-1}}{\gamma_\rho^{-1}}\frac{1}{m^2-m_\omega^2+im_\omega\Gamma_\omega}\right|^2\frac{m_\rho^2}{m^2}, \quad (8)$$

where m is the invariant mass of the lepton pair, $m^2=(p_++p_-)^2$, $A_{\gamma\omega}/A_{\gamma\rho}=\frac{1}{3}$, $\gamma_\omega^{-1}/\gamma_\rho^{-1}=-1.13/3$. The function $\Gamma_\rho(m)$ is given in Eq. (6). The over-all factor m_ρ^2/m^2 in Eq. (8) takes into account the m dependence of the phase space. The function $Y(m)$ has been arbitrarily normalized to unity at $m=m_\rho$ when the ω contribution is absent.

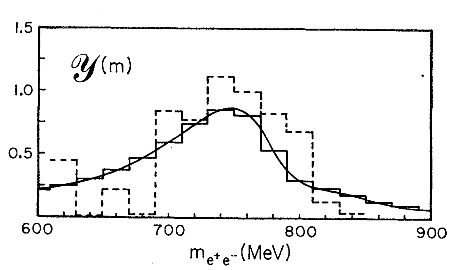

FIG. 5. Graph of the function $\mathcal{Y}(m)$ [see Eqs. (8) and (9)]. The ratio $\gamma_\omega^{-1}/\gamma_\rho^{-1}$ is assumed to be negative. The masses and widths are taken as $m_\rho=765$ MeV, $m_\omega=783.4$ MeV, $\Gamma_{\rho\pi\pi}=125$ MeV, and $\Gamma_\omega=12.6$ MeV. The histogram shows the function binned in 20-MeV intervals. The data of Ref. 9 are shown with dashed lines superimposed upon the function $\mathcal{Y}(m)$.

The function $Y(m)$ has a sharp dip for $m\approx m_\omega$ due to the destructive interference between the ρ and ω. This dip would not be resolvable in an experiment with a resolution comparable to that of Ref. 9, i.e., $\approx\pm15$ MeV/c^2. In order to illustrate more clearly the yield of such an experiment, we define a new function in which we have folded the yield function $Y(m)$ with a Gaussian resolution curve with $\sigma=15$ MeV. Thus the experimentally observed yield should closely resemble

$$\mathcal{Y}(m)=\frac{1}{\sigma(2\pi)^{1/2}}\int_{-\infty}^{\infty}dm'e^{-(m-m')^2/2\sigma^2}Y(m'). \quad (9)$$

This function has been plotted in Fig. 5. Note that the dip near $m\approx m_\omega$ has almost completely disappeared in the "folding" process. The analogous curve for $\mathcal{Y}(m)$ calculated with the VDM, i.e., $A_{\gamma\omega}/A_{\gamma\rho}=\gamma_\omega^{-1}/\gamma_\rho^{-1}$, is

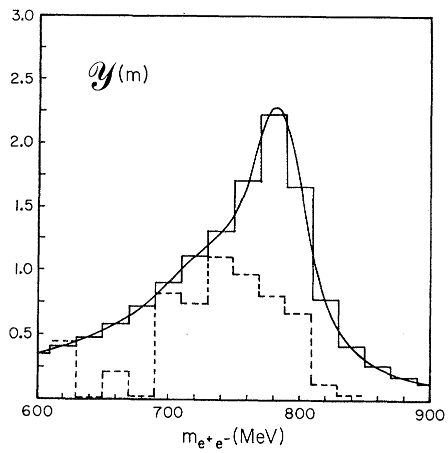

FIG. 6. Graph of the function $\mathcal{Y}(m)$ [see Eqs. (8) and (9)]. The ratio $\gamma_\omega^{-1}/\gamma_\rho^{-1}$ is assumed to be positive. The masses and widths are taken as $m_\rho=765$ MeV, $m_\omega=783.4$ MeV, $\Gamma_{\rho\pi\pi}=125$ MeV, and $\Gamma_\omega=12.6$ MeV. The histogram shows the function binned in 20-MeV intervals. The data of Ref. 9 are shown with dashed lines superimposed upon the function $\mathcal{Y}(m)$.

shown in Fig. 6. The data of Ref. 9 are shown superimposed on Figs. 5 and 6.

Clearly, the VDM calculation agrees less well with the data than the model of Fig. 4. The photon–vector-meson coupling constant appears in the photoproduction amplitude in the above model only linearly (not squared as in the VDM). Since we have assumed that $\gamma_\omega^{-1}/\gamma_\rho^{-1}$ is negative, the ω interferes "destructively," not "constructively" as in the VDM. This changes the effect of the ω from a large increase in the expected yield to a small decrease.

ACKNOWLEDGMENTS

The author wishes to thank Professor Roy Weinstein, Professor T. A. Griffy, and Dr. R. B. Clark for several helpful discussions.